Journal of Engineering and Technology Vol. 3 No. 2, 2004 *ISSN : 1684-4114*

NUMERICAL INVESTIGATION OF NATURAL CONVECTION INSIDE ECCENTRIC HORIZONTAL ANNULUS FILLED WITH SATURATED POROUS MEDIA – VERTICAL ECCENTRICITY

Ahmed F. Alfahaid*

ABSTRACT

A numerical investigation of natural convection inside eccentric annulus filled with saturated porous medium is carried out. The solution scheme is based on two-dimensional model, which is governed by Darcy-Oberbeck-Boussinseq equation. The inner cylinder is heated isothermally while the outer one is cooled isothermally. Discretization of the governing equations is achieved using finite element scheme based on Galerkin method of weighted residuals. The effect of pertinent parameters such as modified Rayleigh number (Ra) and relative eccentricity for radius ratio of 2 are considered in this study. The modified Rayleigh number ranges from 10 to 400 while the relative eccentricity () ranges from 0.1 to 0.8.

The numerical results obtained from the present model are compared with the available published results. An overall good agreement is observed between the current results and the available published results.

1. INTRODUCTION

Natural convection in horizontal porous annuli has a wide variety of technological applications such as insulation of aircraft cabin or horizontal pipes, cryogenics, the storage of thermal energy, and the underground cable systems. The case considered here, probably of the most practical importance in which the cylinder's surfaces are impermeable and maintained at constant uniform temperatures, with the inner temperature being higher than the outer. As a result of temperature difference buoyancy driven flow is induced in the media.

The case of concentric cylinders has received the most attention in the literature. Caltagirone [1] visualized the isotherms in an annulus of radius ratio of 2, and determined experimentally the Nusselt number based on the temperature measurements of the thermal field. At high Rayleigh numbers, the flow was reported to have a change from two-dimensional to three-dimensional oscillatory motion, partially confirmed by finite element simulation, which let the author to conclude that multi-cellular two-dimensional do not exist. In the same study, the equations governing two-dimensional convection motion were solved using finite difference, but due to the insufficient number of grid points Caltagirone was unable to obtain other flow regimes in addition to the two-cellular one. Echigo et al. (2) also obtained two-dimensional steady state numerical results taking into account the radiation effect.

Burns and Tien [3] examined the variations of the overall heat transfer coefficients with the external heat transfer coefficient and radius ratio by steady-state two-dimensional analyses with the finite difference method and purturbation method. It was indicated that a maximum value of overall heat transfer coefficient existed depending upon the radius ratio.

* *Mechanical Technology Department, Riyadh College of Technology, PO. Box 91471, Riyadh 11633, Saudi Arabia*

Using finite difference method Fukuda et al. [4] obtained three-dimensional results using finite difference method for an inclined annulus. However, the results could not be extended to the horizontal case owing to the presence of the gravitational force component in the axial direction of the annulus, which is not present in the horizontal case.

Rao el al. [5-6] investigated steady and transient analyses of natural convection in horizontal porous annulus with Galerkin method. They obtained three families of convergent solutions appearing one after the other with increasing modified Rayleigh number corresponding to different initial conditions. They also determined numerically the bifurcation point, which coincide very well with that from the experimental observations of Caltagirone [1].

Two-dimensional numerical work by Mota et al. [7-9] solved two-dimensional Boussinesq equations using finite difference scheme with an ADI method and successive under relaxation to a very fine grid. They showed that for very small radius ratio and on increasing the Rayleigh number, the steady state regime changes from two to four to six to eight cells without exhibiting a hystresis loop. For radius ratio above 1.75 approximately, closed hystersis loops between ranges containing 2 or 4 cells are obtained.

Charrier-Mojtabi et al. [10], observed the two-dimensional two-cellular flow pattern for radius ratio of 2 when Rayleigh number was increased up to 250, after which three-dimensional effect become visible in the upper part of the annulus region. When Rayleigh number decreases the flow pattern become two-dimensional again and consisted of four convection cell flow structures and seems to confirm the hystresis behavior obtained by Mota and Saatdjian [7-9].

Alfahaid and Sakr [11] studied numerically steady state natural convection in fully saturated porous concentric annuls using Galerkin method. They investigated the effect of modified Rayleigh number and the radius ratio on the Nusselt number at the heated cylinder.

The eccentric annulus was studied numerically by Bau et al., using finite difference and regular perturbation expansion technique [12]. Using a two-term regular perturbation expansion Bau [13] investigated three different geometrical configurations: an eccentric annulus, a buried pipe, and two cylinders one outside the other.

Himasekhar and Bau [14] used boundary layer technique to obtain a correlation for Nusselt number as a function of Rayliegh number and the geometrical parameters valid for a large range of Rayleigh numbers.

Mota and Saatdjian [15] used accurate finite difference code for two-dimensional convection between concentric cylinders and modified it to investigate the flow in eccentric annuli. They used only vertical eccentricity in a range from 0.01 to 0.9 for a radius ratio of 2. They found that the net gain due to eccentricity of insulation could be of order 10% compared with the concentric case. They also, showed that reducing the radius ratio or increasing the eccentricity has the same impact on the geometry in the top part of the layer where the convective effects are more pronounced.

2. Mathematical Formulation

The problem considered here is a porous layer bounded between two horizontal concentric cylinders of radii R_i and R_o as shown in Fig. (1). The surfaces of the two cylinders are assumed to be maintained at a constant temperatures T_i and T_o respectively with T_i T_o. The governing equations for transient natural convection with Boussinesq, Darcy flow, and negligible inertia approximation are given as follows:

$$\nabla.\bar{v} = 0 \tag{1}$$

$$\frac{\mu}{K}\bar{v} = -\left[\nabla p - \rho_f \bar{g}\right] \tag{2}$$

$$(\rho c)_e \frac{\partial T}{\partial t} = \lambda_e \nabla^2 T - (\rho c)\left[\nabla.\bar{v}\,T\right] \tag{3}$$

$$\rho_f = \rho_o\left[1 - \beta_f (T - T_o)\right] \tag{4}$$

By taking the curl of Eq. (2) and using Eq. (4), we obtain the following equations:

$$\nabla^2\psi = -\frac{\rho_f K}{\mu} g\,\rho_o \beta_f \frac{\partial T}{\partial x} \tag{5}$$

$$\nabla^2 T - \frac{c_f}{\lambda_e}\left[\frac{\partial\psi}{\partial y}\frac{\partial T}{\partial x} - \frac{\partial\psi}{\partial x}\frac{\partial T}{\partial y}\right] = \frac{\rho_e c_e}{\lambda_e}\frac{\partial T}{\partial t} \tag{6}$$

where

$$v_x = \frac{1}{\rho_f}\frac{\partial\psi}{\partial y},\quad v_y = \frac{-1}{\rho_f}\frac{\partial\psi}{\partial x} \tag{7}$$

Non-dimensionalizing the variables as defined below;

$$\theta = \frac{T - T_o}{T_i - T_o},\quad x^* = \frac{x}{R_i},\quad y^* = \frac{y}{R_i}$$

$$\psi^* = \frac{\psi}{\alpha\rho_f};\ \text{where } \alpha = \frac{\lambda_e}{\rho_f c_f},\quad t^* = \frac{\lambda_e}{\rho_e c_e}\frac{t}{R_i^2}$$

The governing equations reduce to the following:

$$\nabla^2\theta - \left(\frac{\partial\psi^*}{\partial y^*}\frac{\partial\theta}{\partial x^*} - \frac{\partial\psi^*}{\partial x^*}\frac{\partial\theta}{\partial y^*}\right) = \frac{\partial\theta}{\partial t^*} \tag{8}$$

$$\nabla^2\psi^* = -\mathrm{Ra}\frac{\partial\theta}{\partial x^*} \tag{9}$$

Boundary Conditions

The problem is assumed to be symmetric about the vertical axis, and as a result, only one half of the flow domain will be considered in this analysis. The boundary conditions are handled as follows:-

a- Plane of symmetry:

$$\psi^* = 0,\quad \frac{\partial\theta}{\partial x^*} = 0 \tag{10a}$$

b- Inner cylinder surface

$$\psi^* = 0, \quad \theta = 1.0 \tag{10b}$$

c- Outer cylinder surface

$$\psi^* = 0, \quad \theta = 0 \tag{10c}$$

Heat Transfer

The local Nusselt number at the inner and outer cylinders surfaces can be calculated from the following equations respectively:

$$Nu_i = \frac{\bar{h} R_i}{\lambda_e} = -\left(\frac{\partial\theta}{\partial n}\right)_{x^{*2}+y^{*2}=1} \tag{11a}$$

$$Nu_o = -\left(\frac{\partial\theta}{\partial n}\right)_{x^{*2}+y^{*2}=R} \tag{11b}$$

Where n: represent the direction normal to the cylinder surface.

The steady state average Nusselt number at the inner or outer cylinders surfaces are equals as given by:

$$\overline{Nu_i} = \overline{Nu_o} = \frac{1}{2\pi}\int_0^{2\pi} Nu_o(\gamma)\, d\gamma \tag{12}$$

3. Numerical Solution

The solutions of Eqs. (8) and (9) subject to the boundary conditions specified by Eq. (10) is obtained numerically by using the Galerkin based finite element method [16, 17]. The objective of the finite element is to reduce the system of governing equations into a discretized set of algebric equations. The procedure begins with the division of the continuum region of interest into a number of simply shaped regions called elements. The grid used in the present calculation is illustrated in Fig. (1). The element type which used here is linear triangular element. The approximate expressions of temperature and stream function in an element are given by polynomials in terms of the nodal values and interploation functions. The interploation functions are derived from the assuption of linear variation of temperature and stream function through the element and are given by the following equation:

$$\psi^e = \sum_{m=1}^{3} N_m \Psi_m^* \tag{13a}$$

$$\theta^e = \sum_{m=1}^{3} N_m \theta_m^* \tag{13b}$$

Where;

N_m is the usual interpolation function and is defined by:

$$N_m = \frac{1}{2A}\,(a_m + b_m x^* + c_m y^*) \tag{14}$$

Where;
A is the element area and

$$a_1 = x_2^* y_3 - x_3^* y_2$$
$$b_1 = y_2^* - y_3^* \qquad (15)$$
$$c_1 = x_3^* - x_2^*$$

The other components are given by cyclic permutation of the subscripts in the order 1,2 and 3. If the approximation given by Eq. (13) is substituted in the governing Eqs.(8-9), and the global errors are minimized using the above interpolation functions N_i as weighting functions. After performing the weighted ingration over the domain G and the application of Green's theorem,

This present model can be written in the equivalent forms:

$$[K_1]\{\overset{*}{\ }\} = \{F_1\} \qquad (16a)$$
$$[K_2]\{\ \} = \{F_2\} \qquad (16b)$$

Where;

$$[K_1] = \sum_{e=1}^{E} \int_{G^e} \left(\frac{\partial[N]^T}{\partial\xi} \cdot \frac{\partial[N]}{\partial\xi} + \frac{\partial[N]^T}{\partial\eta} \cdot \frac{\partial[N]}{\partial\eta} \right) dG$$

$$\{F_1\} = \sum_{e=1}^{E} \int_{\Gamma^e} [N]^T \frac{\partial N}{\partial n} d\Gamma$$

and E = total number of elements,
G = bounded domain,
D = domain boundary,

Simiarly $[K_2]$ and $\{F_2\}$ can be written in the same manner. Equations (8) and (9) result in two sets of linear equations which have been solved by Gauss elemination method. The resulting two sets of equations have been solved iteratively through a computer code written here in FORTRAN langauge. The iterative procedure was terminated when the following relative convergence criterion was satisfied:

$$\left| \frac{\psi^{N+1} - \psi^{N}}{\psi^{N+1}} \right| \le 10^{-4}$$

where; N denote the iteration number performed.

4. MODEL VALIDATION

First the code was validated by solving the convection problem of two concentric horizontal cylinders for which solutions are available. The obtained results compared with the available published data. Table 1 shows the average Nusselt Number for different previous researchers. A good agreement is found between the present work and the other researchers.

5. RESULTS AND DISCUSSIONS

Figure (1) shows the contour lines of stream function for relative vertical eccentricity of 0.2 and different Rayleigh numbers having values of 10, 120, and 300 respectively. It is shown from the figure that the flow is composed of two symmetrical cells about the vertical axis and the centers of cells rise upward as Rayleigh number increases. Also, it is depicted from the figure that the intensity of contour lines increases near the walls of the inner and outer cylinders. Also, the values of stream function in both cells are the same but in opposite signs due to direction of flow.

Figure (2) illustrates the isotherms for relative eccentricity of 0.2 and Rayleigh numbers having values of 10, 120, and 300 respectively. It is shown from the figure that, the isotherms are nearly circular at Ra=10. So, the conduction is the dominant mode of heat transfer and as the Rayleigh number increases the convection becomes dominant and it is noted that the intensity of isotherms become larger at the bottom of the inner cylinder and the top of the outer cylinder, indicating more heat transfer rate at these location.

Figure (3) shows the contour lines of stream function for vertical relative eccentricity of 0.5 and different Rayleigh numbers having values of 10, 120 and 300 respectively. Also, it is shown from the figure that, the flow patterns for Ra=10 and 120 is composed of two flow cells and the flow pattern is composed of four cells at Ra=300. In all cases the flow pattern is symmetrical about the vertical axis, also the centers of large cells moves upward as Rayleigh number increases. The corresponding isotherms are illustrated in Fig. (4), from the figure, it is clear that the conduction is the dominant mode of heat transfer of heat transfer at Ra=10, and more intensive lines are above the inner cylinder. As Rayleigh number increases the convective mode plays it role in the heat transfer process. It is clear that there are more intensive isotherms at the bottom of inner cylinder and above the inner cylinder from the outer cylinder.

Also, it is noticed that separation of the thermal boundary layer takes place as Rayleigh number increases and larger stratification, which is denoted by the straight line portions of the isotherms in the wider portion of the annulus takes place.

The same behavior of the flow and heat transfer characteristics for vertical relative eccentricity of 0.7 and Rayleigh number having values of 10, 120, and 300 are illustrated in Figs. (5, 6).

The average Nusselt number at the inner cylinder as a function of the vertical relative eccentricity is depicted in Fig. (7), for different Rayleigh number. It is shown from the figure that as Rayleigh number increases the average Nusselt number increases. Figure (8) shows the heat flow rate as a function of relative eccentricity for different values of Rayleigh numbers. For very small Rayleigh numbers, the heat flow curve has a minimum located at zero eccentricity; this indicates that the concentric insulation is most efficient one for such cases. For higher values of Rayleigh numbers the total heat flow can be reduced by eccentric insulation. The values of relative eccentricity that locates the minimum heat flow rate increases with the increase of Rayleigh number. Figure (9) shows the variation of the average Nusselt number as a function of Rayleigh number for different eccentricity. From the figure, it is shown that the average Nusselt number increases with the increase of Rayleigh number.

6. CONCLUSIONS

The numerical investigation of natural convection inside eccentric annulus filled with saturated porous medium is carried out. An accurate finite element code was developed to solve the two-dimensional Darcy-Boussinesq equations for an eccentric horizontal annulus filled with saturated porous medium. For Ra = 40, the concentric insulation is the most efficient one for radius ratio 2, which is studied in the present work.

REFERENCES

[1] Caltagirone, J.P., 1976, "Thermo-Convective Instability in Porous Medium Bounded By Two Concentric Horizontal Cylinders," J. of Fluid Mechanics, Vol. 76, pp. 337-362.

[2] Echigo, R., Hasegawa, S. Tottori, S., Shimonure, H. and Okamoto, Y., 1978, "An Analysis on the Radiation and Free Convective Heat Transfer in Horizontal Annulus with Permeable Insulators," Proc. 6 th International Heat Transfer Conf., Vol. 3, pp. 385-390.

[3] Burns, P.J. and Tien, C.L., "Natural Convection in Porous Media Bounded by Concentric Spheres and Horizontal Cylinders," Int. J. of Heat Mass Transfer, Vol. 22, pp. 929-939.

[4] Fukuda, K., Takuka, Y. and Hasegawa, S., "Three-dimensional Natural Convection in a Porous Medium Between Concentric Inclined Cylinders", Vol. HTD-8, 1981, ASME, Orlando, FL., pp. 97-103.

[5] Rao, Y.F., Fukuda, K. and Hasegawa, S., "Steady and Transient Analysis of Natural Convection in a Horizontal Porous Annulus with Galerkin Method," ASME J. of Heat Transfer, Vol. 109, 1987, pp. 919-927.

[6] Rao, Y.F., Fukuda, K. and Hasegawa, S., "A Numerical Study of Three-Dimensional Natural Convection in a Horizontal Porous Annulus with Galerkin Method," Int. J. Heat Mass Transfer, Vol. 31, 1989, pp. 695-707.

[7] Mota, J.P.B., and Sattdjian, F., "Natural Convection in Porous Horizontal Cylindrical Annulus," ASME J. of Heat Transfer, Vol. 116, 1994, pp. 621-626.

[8] Mota, J.P.B., and Sattdjian, F., "Natural Convection in Porous Cylindrical Annuli ", Int. J. Num. Methods Heat Fluid Flow, Vol. 5, 1995, pp. 3-12.

[9] Mota, J.P.B., and Sattdjian, F., "On the Reduction of Natural Convection Heat Transfer in Horizontal Eccentric Annuli Containing Saturated Porous Media," Int. J. Num. Methods Heat Fluid Flow, 7 (4), pp. 401-416, 1997.

[10] Carrier-Mojtabi, M.C., Mojtabi, A. Azaiez, M. and Labrosse, G., "Numerical and Experimental Study of multi-cellular Free Convection Flows in an Annular porous Layer", Int. J. Heat Mass Transfer, Vol. 34, 1991, pp. 3061-3074.

[11] AlFahaid, A.F. and Sakr, R.Y., "Numerical Study of Natural Convection Heat Transfer in Horizontal Annuli Containing Saturated Porous media", Second Saudi Technical Conference and Exhibition STCEX 2002, Vol. 3, pp. 68-76.

[12] Bau, H.H. "Thermal Convection in a Horizontal, Eccentric Annulus Containing a Saturated Porous Medium- An Extended Purturbation Expansion", Int. J. Heat Mass Transfer, Vol. 27, pp. 2277-2287, 1984.

[13] Bau, H.H., 1984, "Low Rayleigh Number Thermal Convection in Saturated Porous

Medium Bounded by Two Horizontal Eccentric Cylinders," ASME J. of Heat Transfer, Vol. 106, 1984, pp. 166-175.

[14] Himasekhar, K. and Bau, H. H., "Large Rayleigh Number Convection in a Horizontal Eccentric Annulus Containig Saturated Porous Media", Int. J. Heat Mass Transfer, Vol. 29, 1986, pp. 703-12.

[15] Mota, J.P.B., and Sattdjian, F., "Natural Convection in Porous Horizontal Cylindrical Annulus," ASME J. of Heat Transfer, Vol. 116, 1994, pp. 621-626.

[16] Rao, S. S., The Finite Element Methods in Engineering, Pergamon Press, 1982.

[17] Pepper, D.W., and Heinrich, J.C., The Finite Element Method- Basic Concepts and Applications, Hemisphere Publishing Corporation, 1992.

[18] Facas, G.N., "Natural Convection From a Buried Pipe with External Baffles", Numerical Heat Transfer, Part A, 27:595-609, 1995.

[19] Facas, G.N and Farouk, B. "Transient and Steady State Natural Convection in a Porous Medium between Two Concentric Cylinders", ASME J. Heat Transfer, Vol. 105, pp. 660-663, 1983.

NOMENCLATURE

c	specific heat	β	thermal expansion coefficient
g	gravity vector	γ	circumferential angle
h	heat transfer coefficient	θ	dimensionless temperature
K	permeability	λ	thermal conductivity
Nu	Nusselt number	μ	viscosity
n	normal direction	ρ	density
R	radius ratio, R_O/R_i	ϕ	prosity
R_i	inner cylinder radius	ψ	stream function
R_o	outer cylinder radius*	ψ^*	dimensionless stream function
Ra	Rayleigh number		
T	temperature		**Subscripts**
t	timee	e	ffective
t*	dimensionless time	f	fluid
v	velocity vector	i	inner
x,y	Cartesian coordinates	o	outer or reference
x*,y*	dimensionless Cartesian coordinates	x,y	Cartesian components

Table 1: Comparison of the average Nusselt number for natural convection for convective flow between two concentric cylinders with radius ratio of 2.

	Caltagirone [1]	Rao et al [3]	Bau [12]	Facas [18]	Facas & Farouk [19]	Present Code
Grid size	49x49	10x10	30x44	50x50	25x25	10x18
Ra=50	1.328	1.341	1.335	1.342	1.362	1.317
Ra=100	1.829	1.861	1.844	1.835	1.902	1.865

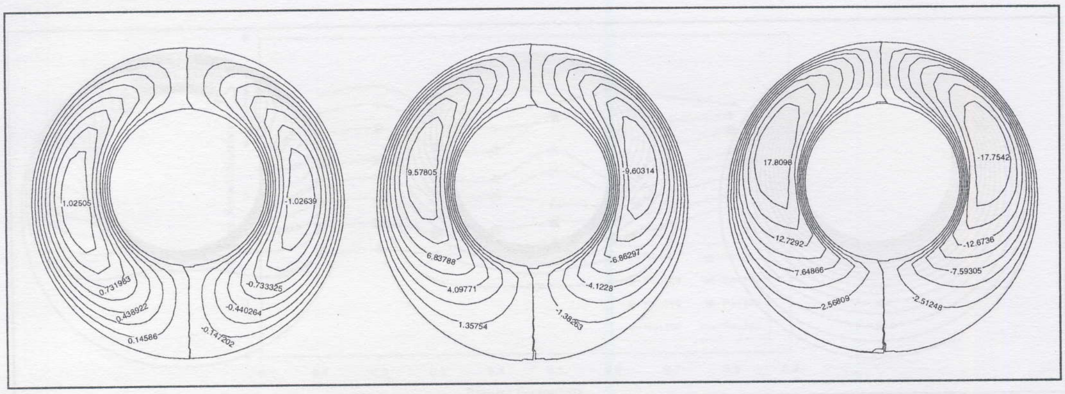

Fig. 1 Stream function contours for relative eccentricity of 0.2 and Rayleigh number of 10, 120 and 300 respectively

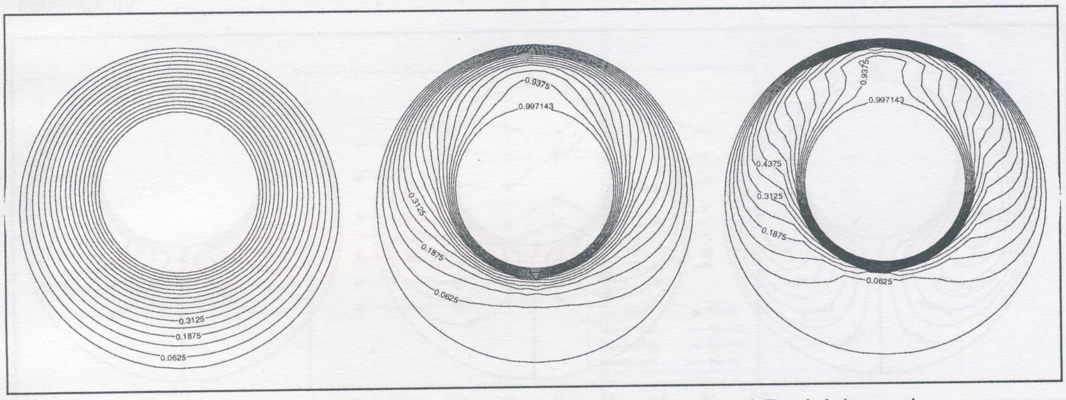

Fig. 2 Isotherms contours for relative eccentricity of 0.2 and Rayleigh number of 10, 120 and 300 respectively

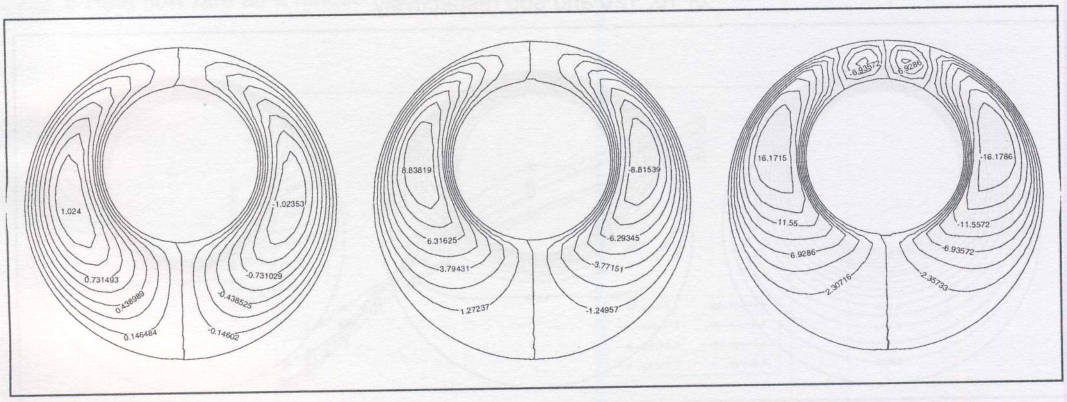

Fig. 3 Stream function contours for relative eccentricity of 0.5 and Rayleigh number of 10, 120 and 300 respectively

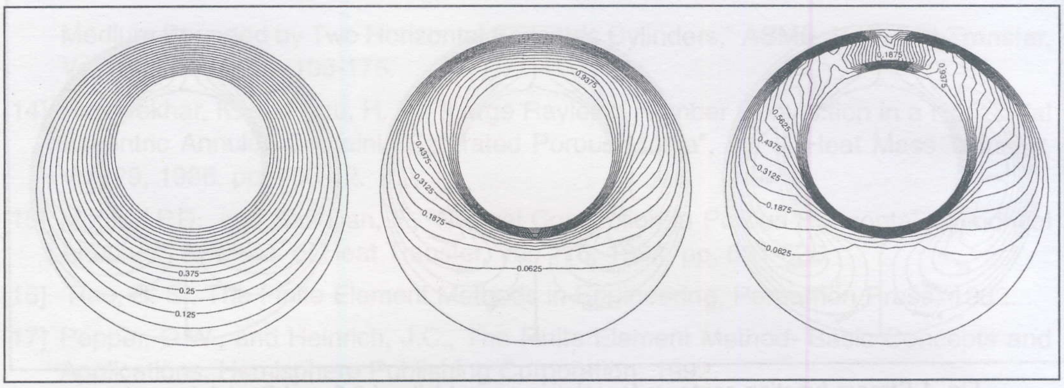

Fig. 4 Isotherms contours for relative eccentricity of 0.5 and Rayleigh number of 10, 120 and 300 respectively

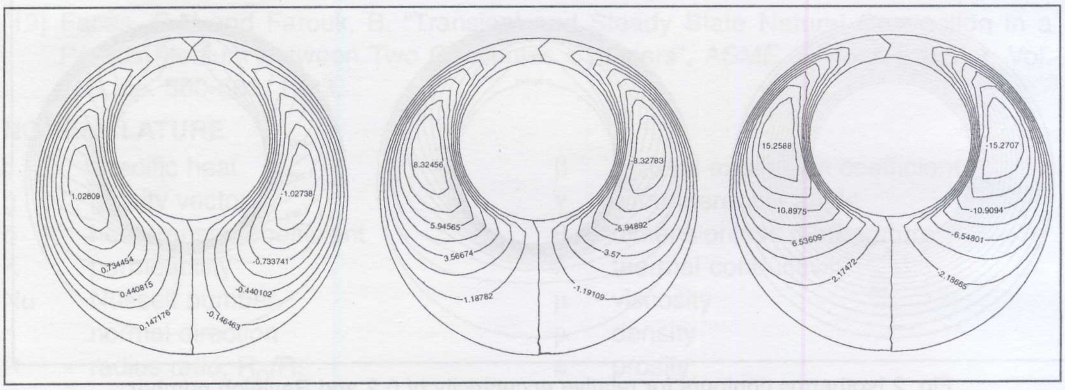

Fig. 5 Stream function contours for relative eccentricity of 0.7 and Rayleigh number of 10, 120 and 300 respectively

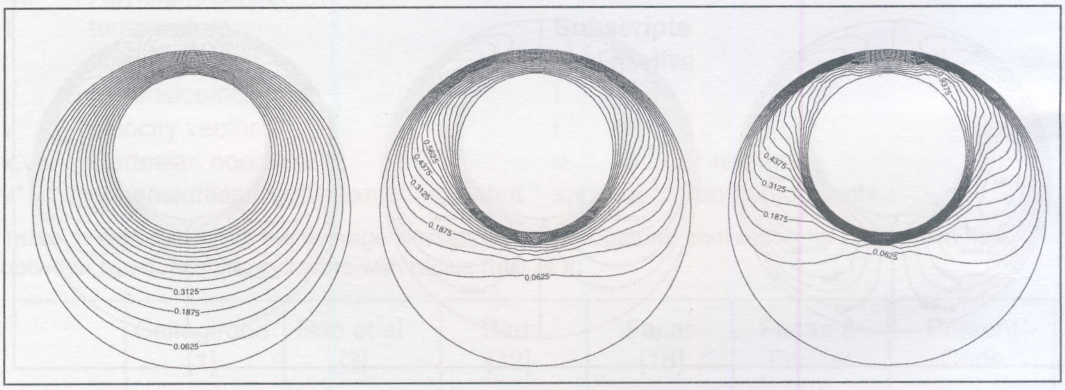

Fig. 6 Isotherms contours for relative eccentricity of 0.7 and Rayleigh number of 10, 120 and 300 respectively

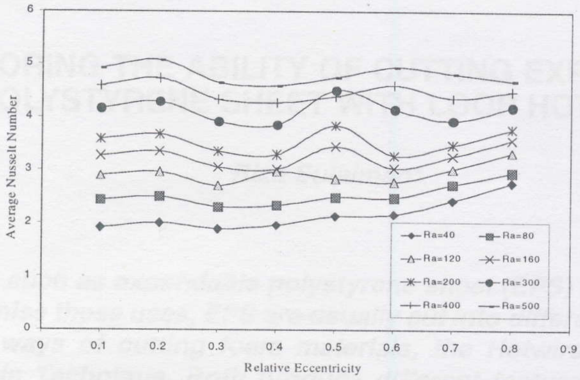

Fig. 7 Average Nusselt number at the inner cylinder as a function of the vertical relative eccentricity.

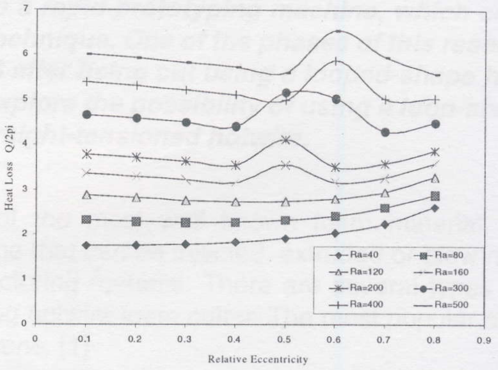

Fig. 8 Heat flow rate as a function of relative eccentricity for different values of Rayleigh numbers.

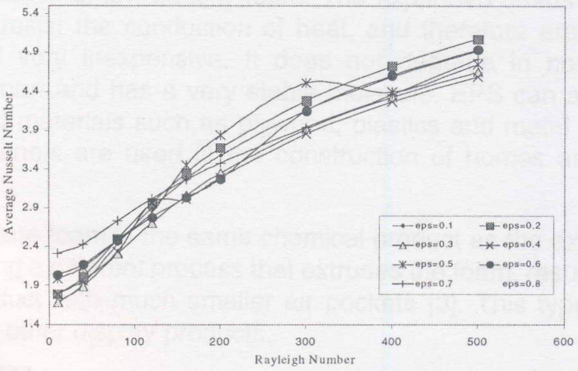

Fig. 9 Average Nusselt number as a function of Rayleigh number for different eccentricity.